Eur. Phys. J. Special Topics **153**, 59–64 (2008)

DOI: 10.1140/epjst/e2008-00393-8

THE EUROPEAN PHYSICAL JOURNAL SPECIAL TOPICS

Photothermal microscopy for studying the role of nano-sized absorbing precursors in laser-induced damage of optical materials

M. Commandré[a], J.-Y. Natoli, and L. Gallais

Institut Fresnel, UMR CNRS 6133, and École Centrale Marseille – Université Paul Cézanne – Université de Provence, Domaine Universitaire Saint Jérôme, 13397 Marseille Cedex 20, France

Abstract. Laser-induced damage in optical components has long been acknowledged as a localized phenomenon linked to the presence of defects. Destructive investigations combined to optical characterizations have led to the conclusion that in high quality components the damage initiators are typically a few nanometers in size and have low densities. The understanding of damage phenomena requires the development of non destructive evaluation techniques with both high spatial resolution and sensitivity to detect these defects. In this context, a High Resolution Photothermal Deflection microscope (HRPD) has been developed and coupled with a damage facility at the same wavelength 1.064 μm. The behavior under irradiation of model defects such as gold inclusions (3 to 250 nm) has been studied. We show how HRPD gives determining information about damage mechanisms.

1 Introduction

Laser-induced damage in case of pulse duration in the nanosecond range has long been acknowledged as a localized phenomenon associated with the presence of defects such as nodules, scratches, fractures, polishing or cleaning residues, metal or dielectric contaminants [1–3]. Absorbing inclusions for example may induce thermal stress initiating damage in the material. With the successive improvements in optical engineering especially on polished and coated surfaces, the damage initiators are no longer detectable by the usual optical methods. Destructive investigations (statistical measurement of damage probability versus energy density, correlated with damage morphology characterization) have led to the conclusion that defects, typically a few nanometers in size, were responsible for laser damage initiation [4–6]. The understanding of damage phenomena requires the development of non destructive tools with both high spatial resolution and sensitivity to study precursors under intensive irradiation. These techniques have to be implemented in damage set-up at the same wavelength for a detailed analysis of damage mechanisms [7]. In this context, Photothermal microscopy (PM) has been widely employed to characterize localized absorption and study the behavior of materials. A High Resolution Photothermal Deflection microscope (HRPD) has been developed and coupled with a damage facility at the same wavelength 1.064 μm [8]. It allows 50 nm-gold inclusions to be detected and studied under illumination. The behavior of model defects such as gold inclusions of different sizes has been studied and experimental results compared with numerical simulations of laser-matter interaction [9,10]. In this paper we first give some information about the size and the density of damage nanoprecursors on optical surfaces. Secondly we quickly present the calculation tools used for absorption and photothermal deflection in case of spherical

[a] e-mail: mireille.commandre@fresnel.fr

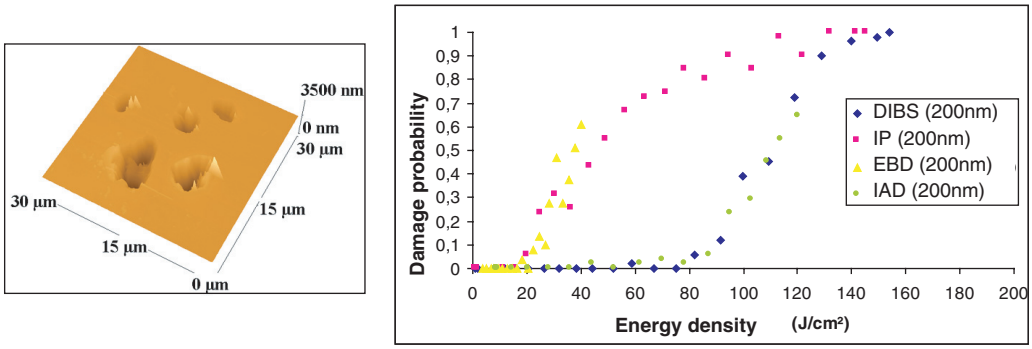

a) b)

Fig. 1. a) AFM image of a damaged area in a silica film. The diameter of the pulsed YAG beam was 100 μm. We observe under the beam 3 to 7 damaged sites in 1000 μm^2, linked to precursor sites. b) Damage probability curves measured at 1064 nm on 200 nm-silica films prepared by different deposition techniques. The order of magnitude of precursor densities calculated from these curves is the same, about 10 precursor sites in 1000 μm^2 or 10^{-2} μm^{-2}.

inclusions. Then the HRPD experimental set-up is described with the method for calibration in term of absorption. At least we present some examples of results obtained with model defects.

2 Density and size of nano-precursors of damage on optical surfaces

Making an absolute measurement of damage probability curves requires perfect control of all experimental parameters and procedures which are described in details elsewhere [11–13]. Thanks to a statistical analysis, damage probability curves can give the density of damage initiators in bulk, on bare surfaces and in thin films [11–13]. We present in fig. 1 an example of result in case of silica thin films. The order of magnitude of the defect density [13] is 10^{-2} defect/μm^2 (fig. 1b). Furthermore this calculated value is corroborated by AFM characterization of damage morphologies (fig. 1a).

The size of these defects has been determined by using an indirect method based on the convergence of several optical data obtained from photothermal measurements and laser-damage probabilities [14]. The size range of precursors is 20–240 nm: metallic ones are close to 20 nm and dielectric close to 200 nm. Because the low values of area density, the mean distance between defects is high compared with the defect size and the defects are isolated. Thus their detection is a single particule problem.

3 Calculation of absorption and modulated temperature distribution in case of spherical absorbing inclusions

The effects of reduction of the pump beam diameter to 1 μm are well-known for photothermal deflection : a strong reduction of the spatial extension of the thermal wave and the photothermal signal is independent on modulation frequency over a large range. In order to have a physical insight of phenomena occurring in optical absorption, thermal diffusion and photothermal deflection, in case of observation of nanoscale objects, it is important to calculate first the electric field around the particle by using Mie theory (figure 2a). By integration of the electric field we can thus calculate the absorption due to the inclusion and by solving the classical heat diffusion equations, obtain the distribution of temperature (fig. 2b). We observe that the thermal wave does not extend beyond a domain related to the absorbing domain (about 5 times the diameter of the inclusion). A consequence is that pump and probe beams have to be focused at the same point with a high precision, inside the absorbing domain.

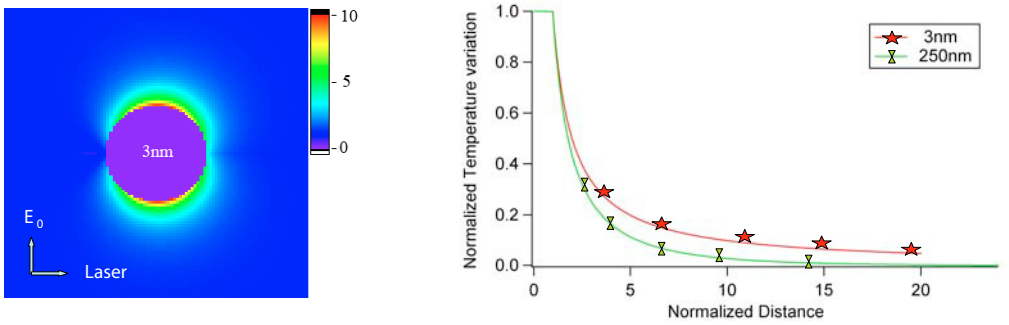

(a) (b)

Fig. 2. (a) Example of calculation of the normalized E-field distribution inside and outside a 3-nm spherical gold inclusion embedded in silica irradiated at 1064 nm with polarization described in figure. This calculation is performed in the plane of incident field, thanks to Mie theory. (b) Normalized modulated temperature distribution inside and outside the inclusion versus normalized distance for two diameters 3 and 250 nm and for modulation frequency 10^6 Hz.

4 High Resolution Photothermal Deflection microscope combined with damage facility and calibration in term of absorption

The microscope (figure 3a) is based on photothermal deflection of the transmitted probe beam: the CW pump beam (1064 nm wavelength) and the probe beam are collinear and focused through the same objective. The diameter of the pump beam on the sample surface is 1 μm. Laser damage thresholds are measured thanks to a pulsed beam (1064-nm wavelength and 6-ns pulse) and the relative spatial positions of beams are controlled by a Nomarski microscope coupled to a CCD camera (not presented in the figure). To control the focalization of both probe and pump beams, translation stages with a precision of 0.1 micrometer have to be used. The experimental system is automated and piezoelectric translation stages with a precision of 10 nanometers permit the 3 axis-movement of the sample. The Nomarski microscope allows easy positioning on a defined area of the sample. We performed calibration of signal when imaging gold nanoinclusions of various diameters by using the usual procedure with a sample of known absorption (titanium implanted silica with adapted dose) and we compared these values with calculations of absorption using Mie theory [30]. We obtained consistent results for calculated and measured values of absorption (fig. 3b).

5 Example of results on model defects such as gold inclusions

With the aim of observing the initiation of damage, engineered defects of nanometric size have been used. In these model samples, different sizes (250, 100 and 3 nm) of calibrated gold inclusions are embedded in ultra-pure silica deposited by evaporation or sputtering. Using an atomic force microscope (AFM), we were able to study the topography of the sample surface. The localization of the gold particles is made by coupling AFM observations and Nomarski microscopy. The height of the dome rising above each inclusion corresponds roughly to the diameter of the inclusion, permitting us to evaluate its size. We have used the HRPD microscope to measure the local absorption change through irradiation [15]. This study permitted us to discriminate between two distinct stages of material modification vs. fluence of irradiation: one detectable at the surface with apparition of cracks (fluence noted Ts) and the second in the neighbourhood of the embedded particle with the decrease of its optical absorption at lower fluence (noted Tp and called “pre-damage” threshold). Fig. 4 describes the pre-damage stage. The evolution of the absorption of several 250 nm gold particles after different single shot laser irradiations is presented. In each case the fluence of the incident beam is less than the laser

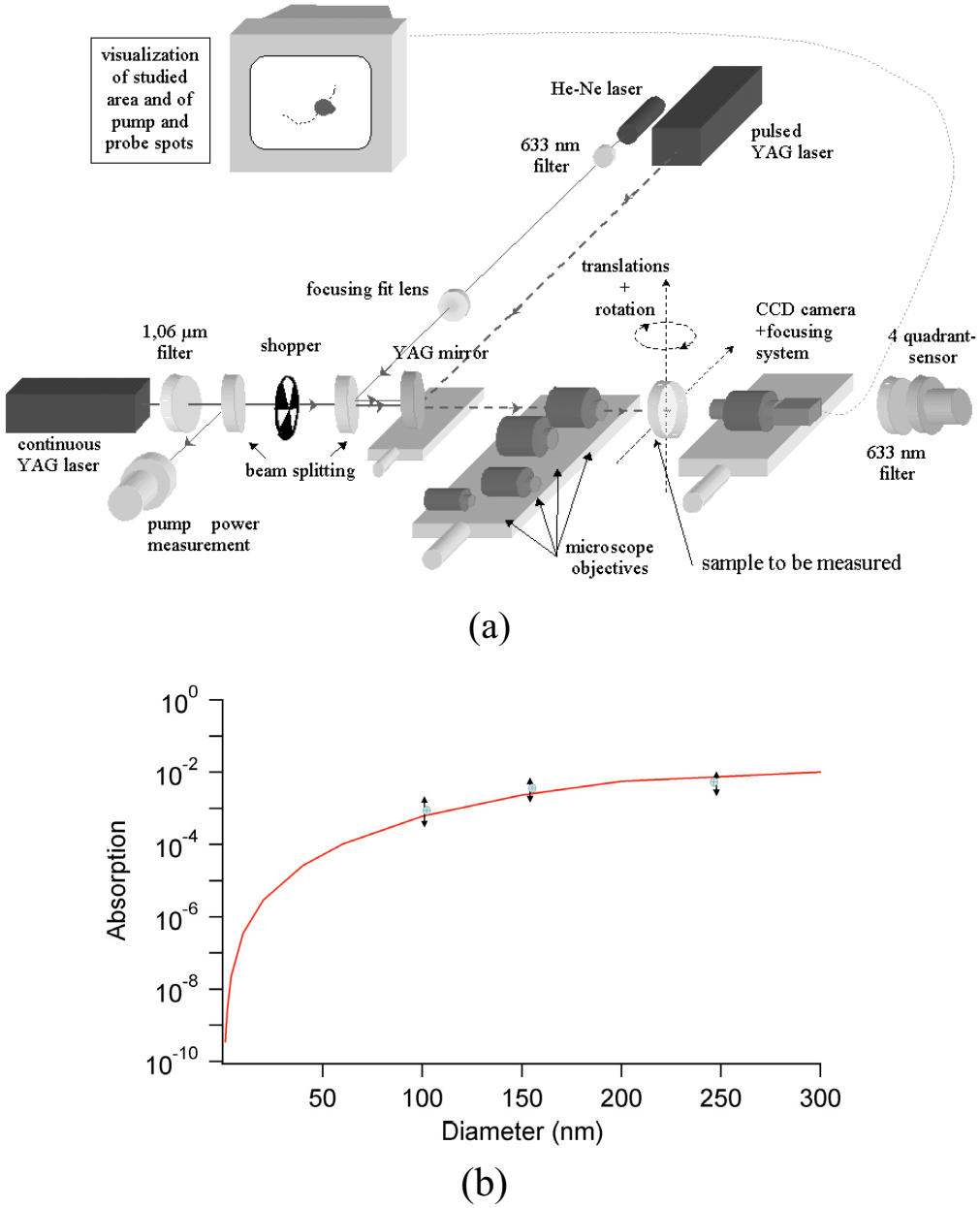

Fig. 3. (a) High resolution photothermal microscope combined with a damage test set-up, both at 1064 nm wavelength. The diameter of the CW YAG laser used as a pump beam for photothermal microscope is 1 μm at the sample surface. (b) Absorption of gold inclusion in silica calculated by Mie theory (continuous line) versus inclusion diameter and measured by photothermal deflection (dots).

damage threshold. In fig. 4a we have the evolution of HRPD images of the different 250 nm-gold inclusions after one shot at the given fluence (from 0.5 to 7.5 J/cm^2). In fig. 4b we present the evolution of the normalized gold inclusion absorption under single shot irradiation, deduced from HRPD images (maximum value of absorption). At low fluence, we can notice that the local absorption of the gold inclusion is constant, at the initial value. When the fluence of irradiation increases, an important and apparently linear decrease of the optical absorption is experimentally observed. In this framework, we may call the intersection of this line with the value 1, the "pre-damage" threshold. We find the result Tp $= 1.5 \pm 0.1$ J/cm^2. In these

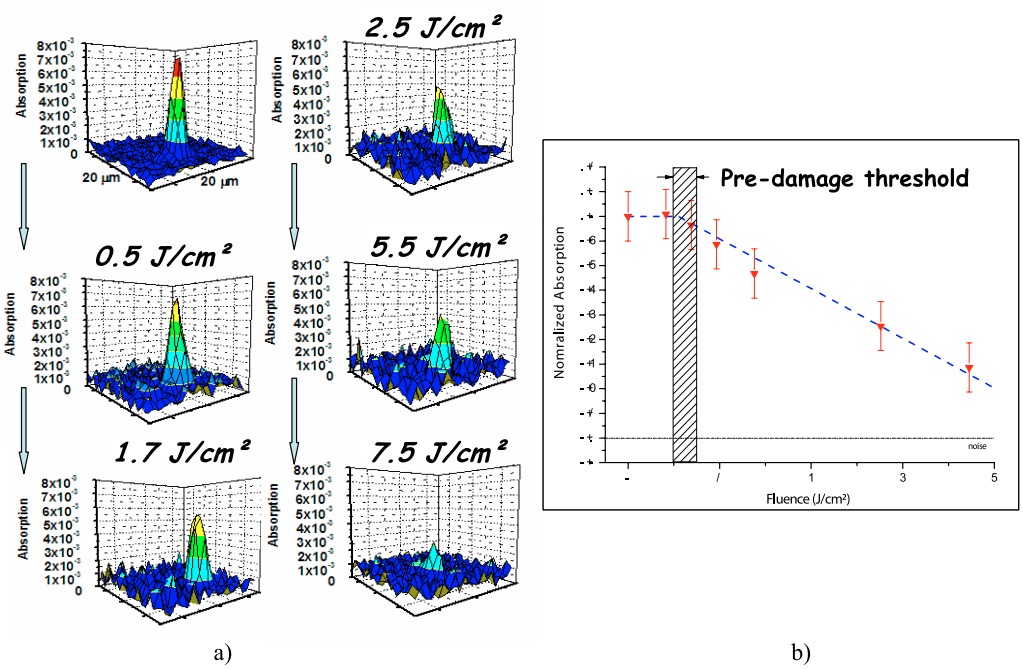

Fig. 4. Pre-damage stage for 250 nm-gold inclusions. a) Evolution of HRPD images of 250 nm-gold inclusions after one shot at the given fluence (from 0.5 to 7.5 J/cm^2). b) Evolution of the gold inclusion absorption under single shot irradiation, deduced from HRPD images.

conditions, the ratio Tp/ Ts is equal to 7. We can notice here that photothermal microscopy allows a quantitative and accurate determination of Tp/Ts. Comparison of this value with numerical simulations show that the pre-damage stage is linked to the melting of the gold inclusion.

The spatial resolution of the HRPD set-up is not sufficient to resolve 3 nm-gold inclusions even in the case of isolated defect. However it is possible to study by this way the damaged sites. Similar study has been performed on 3 nm-samples with an area density of 1 defect/μm^2 and a 30 nm-film thickness. At high fluence (23 J/cm^2) and in case of single shot irradiation we observe a strong change of the material through Nomarski microscope (macroscopic damage). For lower fluences (8 J/cm^2), localized damages appear initiated by the metallic inclusions but the damage density is lower than the inclusion density: the deposited energy is not sufficient to reveal all the model defects. Thus we observe again the "pre-damage" effect through the Nomarski microscope. AFM study shows that pre-damage stage is characterized by a buckling of the film with as mall pit (fig. 5b). In Fig. 5 we present an observation of the damages on the surface by using three different microscopes: Nomarski, atomic force and photothermal deflection. HRPD images show a small increase of absorption in pre-damaged areas only near the borders of the pit. The absorption increases from 10^{-5} (mean value in non irradiated areas) to $4 \cdot 10^{-5}$. In damaged areas the absorption is 10^{-4}. This measured increase of absorption is an experimental proof of the growth mechanism proposed by Papernov [16].

6 Conclusion

A High-Resolution Photothermal Deflection Microscope permits to detect nano-sized absorbing defects responsible of the laser-induced damage. Particularly, the collinear configuration coupled with a reduction of the pump beam diameter to 1 μm allows to study the defects localized in a coating. Currently, metallic inclusions of few tens nanometers can be detected. The use of 3D piezoelectric translation stages permits to obtain a mapping of the optical absorption in the

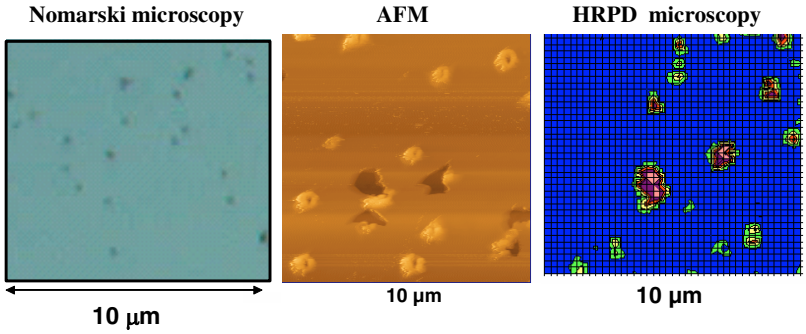

Fig. 5. Case of gold inclusions of diameter 3 nm inserted at a depth of 30 nm with an area density of 1 incl./μm^2. Observation of the damages on the surface by using three different microscopes: Nomarski (a), atomic force (b) and photothermal deflection (c). We observe the small increase of absorption in the flaked regions showing the modification of the surrounding silica.

three directions. It gives images of spatial distribution of absorption and calibration of signal in term of absorption can be performed. Moreover, the coupling with a laser of damage has permitted to study with high accuracy the initiation stage of damage process.

The authors gratefully acknowledge Ph.D. students who were involved in optical characterization, A. During and B. Bertussi and their collaborators from CEA (CESTA, Bruyères-Le-Châtel, LETI, Le Ripault), especially Hervé Bercegol and Jean-Luc Rullier. Funding of this work by CEE, by Région Provence-Alpes-Côte d'Azur, Conseil général Bouches du Rhône and CEA–CESTA is gratefully acknowledged. We also thank Philippe Bouchut from CEA–LETI and LASIM laboratory for preparation of engineered gold defects in silica.

References

1. N. Bloemberger, Appl. Opt. **12**, 661 (1973)
2. T.W. Walker, A.H. Guenther, P. Nielsen, IEEE J. Quantum Electron. **QE-17**, 2053 (1981)
3. M.R. Kozlowski, R.Chow, SPIE **2114**, 640 (1994)
4. J. Dijon, T. Poiroux, C. Desrumeaux, SPIE **2966**, 315 (1997)
5. M.D. Feit, J. Campbell, D. Faux, F.Y. Genin, M.R. Kozlowski, A.M. Robenchik, R. Riddle, A. Salleo, J. Yoshiyama, SPIE **3244**, 350 (1998)
6. S. Papernov, A.W. Schid, J. Anzelotti, D. Smith, Z.R. Chrzan, SPIE **2714**, 384 (1996)
7. A. During, C. Fossati, M. Commandré, Appl. Opt. **41**, 3118 (2002)
8. A. During, M. Commandré, C. Fossati, B. Bertussi, J.-Y. Natoli, J.-L. Rullier, H. Bercegol, P. Bouchut, Opt. Exp. **20**, 2497 (2003)
9. B. Bertussi, J.-Y. Natoli, M. Commandré, J.-L. Rullier, F. Bonneau, P. Combis, P. Bouchut, Opt. Commun. **254**, 299 (2005)
10. B. Bertussi, J.-Y. Natoli, M. Commandré, Appl. Opt. **45**, 1410 (2006)
11. J.-Y. Natoli, L. Gallais, H. Akhouayri, C. Amra, Appl. Opt. **41**, 3156 (2002)
12. L. Gallais, J.-Y. Natoli, C. Amra, Opt. Exp. **10**, 1465 (2002)
13. L. Gallais, Ph.D. thesis, University of Aix-Marseille III, 2002
14. L. Gallais, P. Voarino, C. Amra, J. Opt. Soc. Am. B **21**, 1073 (2003)
15. B. Bertussi, Ph.D. thesis, University of Aix-Marseille III, 2005
16. S. Papernov, A.W. Schmid, J. Appl. Phys. **92**, 5720 (2002)